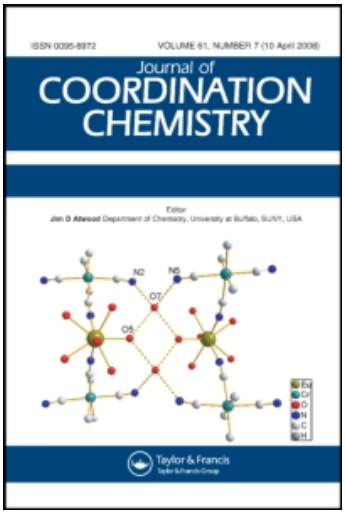

Journal of Coordination Chemistry
Publication details, including instructions for authors and subscription information:
http://www.informaworld.com/smpp/title~content=t713455674

Synthesis, molecular structure, DNA binding and cleavage properties of a novel ternary Cu(II) complex containing dipyrido[3,2-a : 2'3'-c]phenazine and L-tryptophanate

Xue Yi Le[a]; Qin Gu[a]; Zhi Jun Song[a]; Chu Xiong Zhuang[b]; Xiao Long Feng[c]
[a] Department of Applied Chemistry, College of Sciences, South China Agricultural University, Guangzhou, P.R. China [b] College of Life Science, South China Agricultural University, Guangzhou, P.R. China [c] Center of Analysis and Measurement, Zhongshan University, Guangzhou, P.R. China

To cite this Article Le, Xue Yi , Gu, Qin , Song, Zhi Jun , Zhuang, Chu Xiong and Feng, Xiao Long(2007) 'Synthesis, molecular structure, DNA binding and cleavage properties of a novel ternary Cu(II) complex containing dipyrido[3,2-a : 2'3'-c]phenazine and L-tryptophanate', Journal of Coordination Chemistry, 60: 13, 1359 — 1371
To link to this Article: DOI: 10.1080/00958970701394179
URL: http://dx.doi.org/10.1080/00958970701394179

Journal of Coordination Chemistry
Vol. 60, No. 13, 1 July 2007, 1359–1371

Taylor & Francis
Taylor & Francis Group

Synthesis, molecular structure, DNA binding and cleavage properties of a novel ternary Cu(II) complex containing dipyrido[3,2-a : 2′3′-c]phenazine and L-tryptophanate

XUE YI LE*†, QIN GU†, ZHI JUN SONG†,
CHU XIONG ZHUANG‡ and XIAO LONG FENG§

†Department of Applied Chemistry, College of Sciences,
South China Agricultural University, Guangzhou, 510642, P.R. China
‡College of Life Science, South China Agricultural University,
Guangzhou, 510642, P.R. China
§Center of Analysis and Measurement, Zhongshan University,
Guangzhou, 510275, P.R. China

(*Received 2 December 2005; revised 7 July 2006; in final form 11 July 2006*)

A ternary Cu(II) complex with dipyrido[3,2-a : 2′3′-c]phenazine(dppz) and L-tryptophanate (L-trp) has been synthesized and investigated by elemental analysis, molar conductivity, IR and X-ray diffraction. The complex crystallizes in the monoclimic space group $P2_1$ with two molecules in a unit cell of dimensions, $a = 7.949(2)$ Å, $b = 10.724(3)$ Å, $c = 18.580(5)$ Å, $\beta = 93.697(5)^\circ$, $V = 1580.7(8)$ Å^3, $R_1 = 0.0310$, and $wR_2 = 0.0382$. The central copper(II) ion has a distorted square-pyramidal geometry, in which the N,O-donor tryptophanate and N,N-donor heterocyclic base dppz are in the basal plane and a water molecule is coordinated at the axial site. DNA binding properties of the complex were studied by electronic absorption spectroscopy, fluorescence spectroscopy, and viscosity measurement. The DNA cleavage of the complex was investigated by agarose gel electrophoresis. The results show that the complex can bind DNA by intercalation and cleave pBR322 DNA in the presence of ascorbate.

Keywords: Dipyrido[3,2-a : 2′3′-c]phenazine(dppz); L-Tryptophanate; Copper(II) complex; Crystal structure; DNA binding

1. Introduction

Interactions of transition metal polypyridine (2,2′-bipyridine, 1,10-phenanthroline and their derivatives) complexes with DNA have been a topic of interest in biochemical and coordination chemical research, developing DNA structure probes, DNA-dependent electron transfer probes, DNA footprinting and sequence-specific cleaving agents, and so on [1–9]. Transition metal polypyridyl complexes interact with double-stranded DNA in a number of ways [4–6], but in most cases it is non-covalent with intercalation of planar aromatic molecules between the base pairs of the DNA helix. Redox-active $Cu(phen)_2^{2+}$ and the related Cu(II) complexes with substituted phen rings inhibit the

*Corresponding author. Email: lexy@scau.edu.cn

ISSN 0095-8972 print/ISSN 1029-0389 online © 2007 Taylor & Francis
DOI: 10.1080/00958970701394179

activities of DNA or RNA polymerase and induce strand scission of DNA in the presence of H_2O_2 and/or other reductants [10]. However, few studies have been devoted to investigation of DNA binding and cleavage by Cu(II) complexes containing polypyridine and a second amino acid as ligands [11–13].

Studies on DNA binding and cleavage of Cu(II) complexes with amino acids and/or peptide ligands are of great scientific and technological importance. Various side groups of amino acids have potential to recognize the specific base sequence through hydrogen bond formation with the nucleic bases in DNA [14]. The systems act as models of protein–DNA and peptide-derived antitumor agent–DNA interactions. Moreover, Cu(II) complexes with an amino acid and/or a peptide ligand exhibit high superoxide dismutase (SOD) activity [15], and SODs at high concentrations may have the function as peroxidase and enhance H_2O_2-induced DNA damage [16]. It has been found that the polypyridine Cu(II) complexes containing amino acid ligand can serve as a new type of DNA sequence-specific cleaving agent and antitumor agent; incorporation of amino acids in a polypyridine-copper(II)-amino acid system could increase the selectivity of intercalation with DNA [11, 12]. How the polypyridine Cu(II) complexes with amino acid and/or peptide ligands affect DNA-binding and DNA cleavage is a significant subject for in-depth investigation.

In this work, $[Cu(dppz)(L\text{-trp})(H_2O)]ClO_4 \cdot C_2H_5OH \cdot H_2O$, where dppz = dipyrido[3,2-a : 2′3′-c]phenazine whose intercalative plane is larger than that of phen [11, 12] or TATP [13], and L-trp = L-tryptophanate group with an electron-rich indole ring which may contribute to molecular recognition [17], has been synthesized and investigated by elemental analysis, molar conductivity, IR, and single crystal X-ray diffraction methods. The binding and cleavage properties of the complexes to DNA were studied by electronic absorption spectroscopy, fluorescence spectroscopy, viscosity measurement, and agarose gel electrophoresis methods. The results indicated that the complex exhibits DNA binding ability and cleavage activity.

2. Experimental

2.1. *Materials and instrumentation*

Dppz was prepared according to the literature [18], other chemicals were of reagent grade and used without further purification. Calf thymus DNA(CT-DNA) was purchased from Sigma Chemical Company. Solutions of DNA in 5×10^{-3} M Tris-HCl, 5×10^{-2} M NaCl buffer (pH = 7.2) gave a ratio of UV absorbance at 260 and 280 nm of 1.8–1.9 : 1, indicating that the DNA was sufficiently free of protein [19]. After dilutions CT-DNA concentration per nucleotide phosphate, NP, was determined by UV absorbance at 260 nm. The molar absorption coefficient of the DNA at the wavelength was taken as $6600\ M^{-1}\,cm^{-1}$ [20]. The DNA stock solutions of 5 mM were stored at 4EC and used within four days after their preparation. The pBR322 DNA was purchased from Sangon (Canada) Biotechnology Company and dissolved in TBE buffer (4.5×10^{-2} M Tris + 4.5×10^{-2} M H_3BO_3 + 10^{-3} M EDTA, pH = 8.3).

Microanalysis (carbon, nitrogen and hydrogen) was carried out on a Perkin-Elmer 240C microanalyzer; molar conductivity measurement was performed in ethanol with a DDS-11A conductivity gauge. The infrared absorption spectrum in KBr disks was

measured in the 4000–400 cm^{-1} range with a Nicolet 170SX spectrophotometer. The electronic absorption spectra were recorded on a Pharmacia 4000 UV-Vis spectrophotometer.

2.2. *Synthesis*

The complex was prepared by reaction of $Cu(ClO_4)_2 \cdot 6H_2O$ (1 mmol) and dppz (1 mmol) in 10 mL of 50% (v/v) aqueous ethanol, followed by the addition of 5 mL of aqueous solution of L-tryptophan (1 mmol) and NaOH (1 mmol). The solution was stirred for about 30 min at ambient temperature and filtered. The resulting solution was left to evaporate at room temperature. Dark blue crystals, suitable for X-ray studies, formed after a month. The crystals were filtered and air-dried. Yield: 89%. Microanalysis: Calcd for $C_{31}H_{31}ClCuN_6O_9$: C, 50.96; H, 4.28; N, 11.51. Found: C, 50.29; H, 4.23; N, 11.72.

Caution! Perchlorate compounds are potentially explosive and should be handled carefully.

2.3. *X-ray structural determination*

A single crystal ($0.36 \times 0.18 \times 0.12\,mm^3$) of the complex was selected for X-ray diffraction measurement on a Bruker Smart 1 K CCD system diffractometer with graphite monochromated Mo-Kα radiation at $\lambda = 0.71073$ Å. The SMART program was applied to determine cell parameters, and the collected data were reduced using the SAINT+ program [21]. Absorption corrections were applied with the Siemens Area Detector ABSorption (SADABS) program [22]. Details of the structure solution and refinement for the complex are shown in table 1.

The structure was solved by direct and Fourier methods, and refinements were carried out by full-matrix least squares on F^2 with positional and anisotropic thermal parameters. The atomic coordinates and anisotropic thermal parameters for non-hydrogen atoms were refined to convergence. All hydrogen atoms were placed in calculated positions. Atomic scattering factors were taken from International tables for X-ray Crystallography [23]. All calculations were performed on a PC with the Siemens SHELXS97 [24] and SHELXL97 [25] program packages. Selected bond distances and angles are listed in table 2.

2.4. *DNA binding studies*

2.4.1. Electronic absorption titration. In order to obtain the intrinsic binding constant K_b for the interaction of the complex with CT-DNA, the absorption at 258 nm of $[Cu(dppz)(L\text{-trp})(H_2O)]ClO_4 \cdot C_2H_5OH \cdot H_2O$ (2.0×10^{-5} M) was recorded by differential procedure before and after addition of CT-DNA in the 5×10^{-3} M Tris-HCl/5×10^{-2} M NaCl buffer (pH = 7.2).

2.4.2. Fluorescence spectra. Fluorescence spectra were recorded on F-4500 fluorescence spectrophotometer at room temperature with excitation at 525 nm and

Table 1. Crystallographic data of the complex.

Chemical formula	$C_{31}H_{31}ClCuN_6O_9$
F_w	730.61
Temperature (K)	293(2)
Crystal size (mm^3)	$0.36 \times 0.18 \times 0.12$
Space group	$P2_1$
Crystal system	Monoclinic
Unit cell dimensions (Å, °)	
a	7.949(2)
b	10.724(3)
c	18.5810(5)
β	77.813(5)
V (Å^3)	1580.7(8)
Z	2
D_c (g cm^{-3})	1.535
μ (mm^{-1})	0.841
$F(000)$	754
θ range for data collection (°)	1.10–27.03
Limiting indices	$-9 \le h \le 9$, $-15 \le k \le 15$, $-15 \le l \le 15$
Reflections collected/Unique	10770/6676 ($R_{int} = 0.0171$)
Max and min transmission	0.9058, 0.7517
Refined parameters	433
Goodness of fit on F^2	1.064
Final R indices [$I > 2\sigma(I)$]	$R_1 = 0.0310$, $wR_2 = 0.0790$
R indices (all data)	$R_1 = 0.0382$, $wR_2 = 0.0903$
Absolute structure parameter	0.021(10)
Max., min. height in final ΔF map (e Å^{-3})	0.375, −0.280

$w = 1/[\sigma^2(F_o^2) + (0.0471P)^2 + 0.0000P]$, where $P = (F_o^2 + 2F_c^2)/3$.

Table 2. Selected bond lengths (Å) and angles (°) for the complex.

Cu(1)–O(2)	1.929(2)	Cu(1)–N(5)	1.992(2)
Cu(1)–N(1)	2.004(2)	Cu(1)–N(2)	2.004(2)
Cu(1)–O(8W)	2.3144(19)	N(5)···O(1)[a]	3.003(3)
O(2)–Cu(1)–N(5)	84.07(8)	O(2)–Cu(1)–N(1)	92.80(10)
N(5)–Cu(1)–N(1)	156.45(9)	O(2)–Cu(1)–N(2)	174.87(9)
N(5)–Cu(1)–N(2)	100.76(10)	N(1)–Cu(1)–N(2)	82.09(8)
O(2)–Cu(1)–O(8W)	88.44(10)	N(5)–Cu(1)–O(8W)	99.57(9)
N(1)–Cu(1)–O(8W)	103.68(10)	N(2)–Cu(1)–O(8W)	92.42(10)

Symmetry transformations used to generate equivalent atoms: a: $-x+1$, $y+1/2$, $-z+1$.

emission at 600 nm. The experiment was carried out by titrating the complex (1.2×10^{-3} M in 5×10^{-3} M Tris-HCl/5×10^{-2} M NaCl buffer) into solutions containing 5.5×10^{-6} M CT-DNA and 4.9×10^{-6} M ethidium bromide.

2.4.3. Viscosity measurement. Viscosity measurements were carried out on an Ubbelodhe viscometer maintained at a constant temperature [29(±0.1)EC] in a thermostatic bath. Data were presented as $(\eta/\eta_0)^{1/3}$ *versus* [complex]/[DNA], where η and η_0 are specific viscosities of DNA solutions in the presence and absence of the complex, respectively. The relative specific viscosity values were calculated according to the relation $\eta = (t - t_0)/t_0$, where t refers the flow time of DNA solutions in the presence and absence of the complex, and t_0 is the flow time of buffer alone.

2.5. *DNA cleavage*

The cleavage of plasmid DNA was determined by agarose gel electrophoresis. A typical gel electrophoresis experiment was performed by incubation for 5 min of 300 ng pBR322 DNA, 4 μM complex/dppz/Cu^{2+}, 200 μM ascorbate in Tris-HCl/NaCl buffer to yield a total volume of 20 μL. After incubation, samples were electrophoresed for 40 min at 100 V on 0.8% agarose gel in TBE buffer (4.5×10^{-2} M Tris + 4.5×10^{-2} M $H_3BO_3 + 10^{-3}$ M EDTA, pH = 8.3). The gel was then stained using Gold View (4–5 μL) and photographed on BIO-RAD GEL DOC. The concentration of the complex was also varied from 1 to 9 μM while keeping the concentration of ascorbate 50 times higher than that of the complex. In the inhibition reactions, DMSO (4 μL) was initially added to pBR322 DNA (300 ng), and incubated for 15 min prior to the addition of the complex (4 μM) and ascorbate (200 μM). The mixture was diluted with the buffer to a total volume of 20 μL. After a further incubation of 5 min, the sample was subjected to gel electrophoresis as abore. Densitometric quantification was performed using gel analysis software Quantity One-4.1.0, Bio-Rad Laboratories, USA.

3. Results and discussion

3.1. *General aspects*

The elemental analyses for the complex are in good agreement with the following formula: $[Cu(dppz)(L\text{-trp})(H_2O)]ClO_4 \cdot C_2H_5OH \cdot H_2O$. The complex is soluble in methanol and ethanol, but not in ether and other less polar organic solvents. Molar conductivity measurement in ethanol indicates a 1 : 1 electrolyte value [26] ($\Lambda = 28.8\ S\,cm^2\,mol^{-1}$).

3.2. *Crystal structure*

The structure analysis indicates that the complex crystallizes in the monoclinic space group $P2_1$ with two $[Cu(dppz)(L\text{-trp})(H_2O)]^+$ molecules in the unit cell. Each Cu(II) ion is coordinated to two nitrogen atoms of dppz and the amino nitrogen and one carboxylate oxygen of L-trp [Cu(1)–O(2) = 1.929(2), Cu(1)–N(5) = 1.992(2), Cu(1)–N(1) = 2.004(2), and Cu(1)–N(2) = 2.004(2) nm], one water oxygen at an axial position [Cu(1)–O(8W) = 2.3144(19) nm], the resulting coordination geometry is a distorted square pyramid (figure 1), where N(5), N(1), N(2), O(2) and Cu atoms for the complex deviate by −0.1883, −0.2036, 0.1879, 0.2040, and 0.2082 Å, respectively, from the least-squares plane ($5.518x - 0.460\ y - 12.491\ z = 8.6363$) defined by the four ligating atoms N(5), N(1), N(2), O(1), and Cu indicating that the five atoms in the equatorial positions are approximately coplanar. Selected bond lengths and angles for the complex are comparable to those observed for similar complexes [15, 27, 28]. The bond angles observed around the central Cu atoms range from 82.09(8)–100.76(10)° in the equatorial positions and from 88.44(10)–103.68(10)° in the apical positions, showing the angle variability in the geometry adopted by five-coordinate Cu(II) complexes. The carboxyl group of the amino acid is coordinated to the Cu(II) *via* one oxygen as a unidentate group, in which the bond distance [1.271(4) Å] between the coordinated oxygen atom and the carbon atom is slightly longer than that [1.236(3) Å]

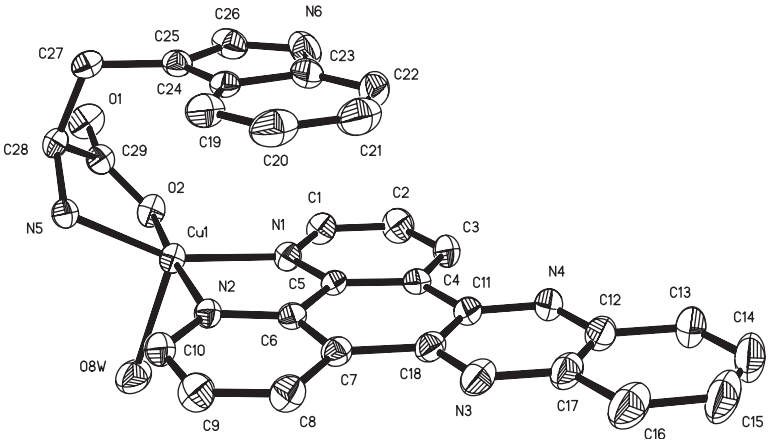

Figure 1. ORTEP plot showing the structure of $[Cu(dppz)(L\text{-trp})(H_2O)]^+$ cation and the atom-numbering scheme.

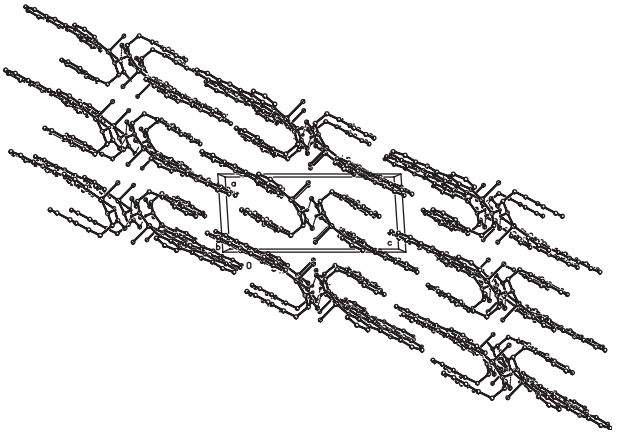

Figure 2. Packed structure along *a*-axis (bottom) for $[Cu(dppz)(L\text{-trp})(H_2O)]ClO_4 \cdot C_2H_5OH \cdot H_2O$.

between the uncoordinated oxygen atom and the carbon atom, indicating electron delocalization in the carboxyl group. An intermolecular hydrogen bond exists in the crystal of the complex, and the $D \cdots A$ separation is 3.003(3) Å for $N(5) \cdots O(1)$; the $D \cdots H \cdots A$ angle is ca 132.9° for N(5)–H(5A)–O(1) (symmetry code: $-x+1$, $y+1/2$, $-z+1$). In addition, the most interesting structural feature of the complex is the existence of the intramolecular and intermolecular stacking interactions between the aromatic rings of L-trp and dppz with average spacings of 3.4049 and 3.3703 Å, respectively. The interactions are similar to the stacking interaction between neighboring DNA bases in the direction of the molecular axis in the DNA double helices, and make the complex form a supramolecular configuration (figure 2).

3.3. *Infrared absorption spectrum*

The IR spectrum of the complex further reflects the structural features found by X-ray analysis. The strong and wide band near 3420 cm^{-1} are ascribed to the stretching

vibrations of the coordinated and crystalline water molecules. The bands at 3314 and 3255 cm^{-1} can be attributed to the stretching vibrations of the coordinated NH_2 group. The absence of any band in the region 1750–1700 cm^{-1} in the IR spectrum of the isolated complex suggests coordination of the COO^- group of L-trp to Cu(II). The bands at 1637 and 1400 cm^{-1} can be attributed, respectively, to the antisymmetric and symmetric stretching vibrations of the coordinated carboxylate of which the difference value [$\nu_{as}(COO^-) - \nu_s(COO^-) = 237\,cm^{-1}$] is consistent with unidentate coordination of the carboxyl group [29]. Thus, one can deduce that the monovalent anion of L-trp is coordinated to the metal ion as a bidentate N,O-ligand, which is in good agreement with the result obtained by X-ray diffraction. The band at 1601 cm^{-1} is assigned to the stretching vibration of the C=N group of the dppz ligand, confirming its coordination to the metal ion [30].

3.4. *DNA binding studies*

Binding of transition metal complexes to DNA has been the subject of interest for development of effective chemical nucleases. In this work, the binding properties of the complex to calf thymus DNA were studied by electronic absorption spectroscopy, fluorescence spectroscopy and viscosity measurement.

3.4.1. Electronic absorption spectroscopy. The broad and weak absorption band at 621 nm (higher energy) [$\varepsilon = 75\,L\,mol^{-1}\,cm^{-1}$] of the complex under the experimental conditions can be attributed to the d–d transition of the central Cu^{2+} ion, indicating that the complex may have a distorted square-pyramidal geometry [31], as observed in the solid state.

The electronic absorption spectra of the complex in the absence and presence of CT-DNA in the range of 225–350 nm are given in figure 3. The complex exhibits a very strong band at 256 nm which can be attributed to the $\pi \rightarrow \pi^*$ transition of the dppz ligand. The absorption peak intensity of the complex decreases remarkably with the increase in concentration of DNA, which indicates binding of the complex to DNA by intercalation [30]. Based on the L-trp ligand with a negative charge and the smaller area compared with the co-planar dppz ligand (as shown in figure 1), we speculate that $[Cu(dppz)(L\text{-}trp)(H_2O)]^+$ binds to DNA by insertion of dppz ligand into adjacent base pairs on the DNA duplex.

In general, the extent of the hypochromism is consistent with the strength of intercalative interaction. The intrinsic binding constant K_b was calculated according to the following equation:

$$\frac{[DNA]}{\varepsilon_a - \varepsilon_f} = \frac{[DNA]}{(\varepsilon_b - \varepsilon_f) + 1/K_b(\varepsilon_b - \varepsilon_f)}$$

where [DNA] is the concentration of DNA, ε_a, ε_f and ε_b are the apparent extinction coefficient (A_{obsd}/[M]), the extinction coefficient for the free metal complex, and the extinction coefficient for the metal complex [M] in the fully bound form, respectively. By plotting $C_{DNA}/(\varepsilon_a - \varepsilon_f)$ *versus* C_{DNA}, K_b can be obtained by the ratio of the slope to the intercept of the linear plot [32]. The binding constant K_b of $4.97 \times 10^3\,M^{-1}$ was obtained from the plot of $[DNA]/(\varepsilon_B - \varepsilon_F)$ *versus* [DNA] (inset of figure 3) using

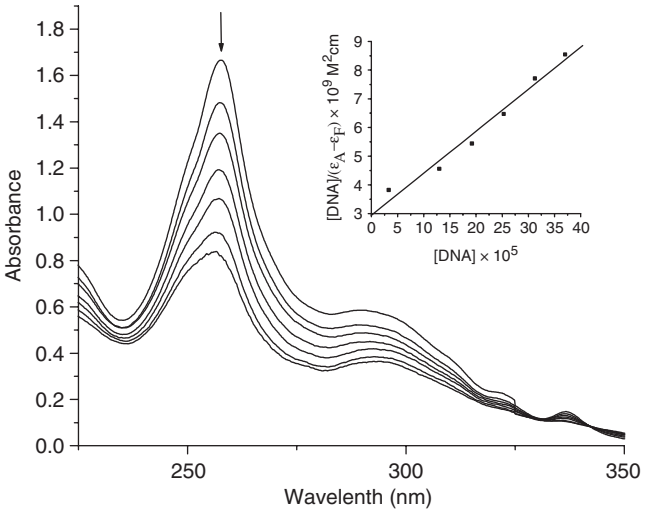

Figure 3. Electronic absorption spectra of $[Cu(dppz)(L\text{-trp})(H_2O)]ClO_4 \cdot C_2H_5OH \cdot H_2O$ (30 μM) in the buffer (5×10^{-3} M Tris-HCl + 5×10^{-2} M NaCl, pH = 7.2) upon addition of CT-DNA at room temperature. [DNA] = 0–400 μM; arrow shows the absorbance change upon increase of DNA concentration. Inset: plot of $[DNA]/(\varepsilon_A - \varepsilon_F)$ *vs.* [DNA].

the absorption at 256 nm, which is smaller than that observed for [Cu(phen)(L-thr)$(H_2O)]^+$ [12], not expected for the larger intercalative plane of dppz compared to phen. This may be because the intramolecular dppz-indole ring stacking interaction in the complex [Cu(dppz) (L-trp) $(H_2O)]^+$ (figure 1), hinders the intercalation of the dppz plane to DNA.

3.4.2. Fluorescence spectroscopy. Ethidium bromide (EB) emits intense fluorescence in the presence of CT DNA due to its strong intercalation between the adjacent DNA base pairs, but a competitive binding of one complex to the DNA would result in the displacement of the bound EB, leading to a reduction in the emission intensity, due to fluorescence quenching of the free EB molecules in aqueous medium [33, 34]. Therefore, the extent of fluoresence quenching for EB bound to DNA is used to determine the extent of binding between another molecule and DNA. Figure 4 shows that the emission intensity of CT–DNA–EB decreases remarkably with addition of the complex, indicating that the complex can replace EB in the CT–DNA–EB system and bind to DNA by intercalation.

The classical Stern–Volmer equation [35], is

$$\frac{I_0}{I} = 1 + K_{sq}r$$

where I_0 and I represent the fluorescence intensities in the absence and presence of the complex, respectively, and r is the concentration ratio of the complex to DNA. K_{sq}, a linear Stern–Volmer quenching constant dependent on the ratio of the bound concentration of EB to the concentration of DNA, whose size can be indicative of the strength of the intercalative interaction of the complex to DNA, can be obtained from

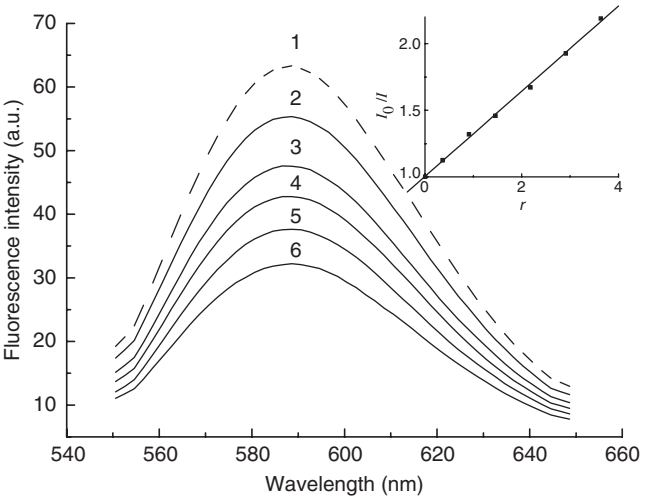

Figure 4. Fluorescence spectra of the binding of EB to DNA in the absence and presence of increasing amounts of the complex, $\lambda_{ex} = 525$ nm, $C_{EB} = 4.9\,\mu M$, $C_{DNA} = 5.5\,\mu M$, $C_{complex}$ (μM): (1) 0, (2) 2, (3) 5, (4) 8, (5) 12, (6) 16. The inset is a Stern–Volmer quenching plot.

linear regression of I_0/I with r. From the inset in figure 4, the K_{sq} value for the complex is 0.32, which is smaller than that (0.41) observed for $[Cu(L\text{-phe})(TATP)(H_2O)]^+$ [13], not as expected from the larger intercalative plane dppz compared to TATP. This also may be from intramolecular dppz-indole ring stacking interaction in $[Cu(dppz)(L\text{-trp})(H_2O)]^+$ is disadvantageous to the intercalation of the dppz plane to DNA, consistent with the above result obtained by electronic absorption spectroscopy.

3.4.3. Viscosity measurement. Further study on the interaction between the complex and DNA was carried out by viscosity measurements. Viscosity experiment (hydrodynamic measurements) can be regarded as one of the least ambiguous and the most critical tests of molecular binding in solution in the absence of crystallographic structural data [36, 37]. The classical intercalative binding of a complex to DNA would causes a significant increase in viscosity of DNA solution due to the increase in separation of base pairs at intercalation sites and hence an increase in overall DNA length. In contrast, a partial and/or non-classical intercalation of a complex to DNA could bend (or kink) the DNA helix, which makes its effective length and viscosity decreased [19]. The values of $(\eta/\eta_0)^{1/3}$ are plotted against [Cu]/[DNA] in figure 5. The results show that the viscosity of DNA increases with the concentration of the complex, indicating a classical intercalation model of the complex to DNA, which is in good agreement with the results of electronic absorption and fluorescence spectroscopies.

3.4.4. Cleavage of pBR322 DNA. The ability of the complex to induce DNA cleavage has been studied by gel electrophoresis using supercoiled pBR322 DNA (4.5×10^{-2} M Tris + 4.5×10^{-2} M H_3BO_3 + 10^{-3} M EDTA, pH = 8.3) in the presence of ascorbate.

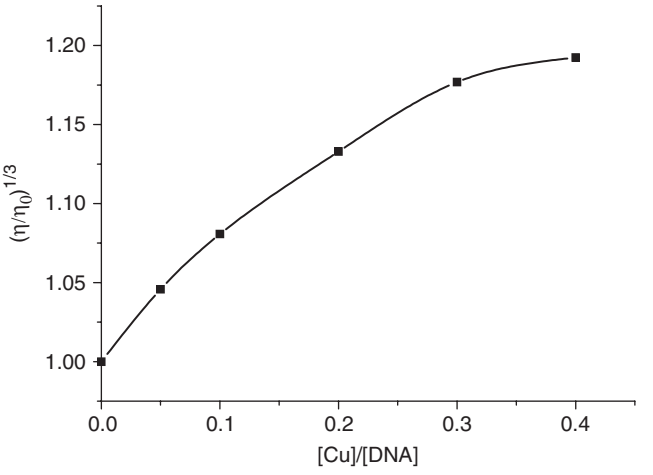

Figure 5. Effect of increasing amounts of $[Cu(dppz)(L\text{-trp})(H_2O)]ClO_4 \cdot C_2H_5OH \cdot H_2O$ on the relative specific viscosity of CT-DNA at 29(±0.1)EC; [DNA] = 0.2 mM.

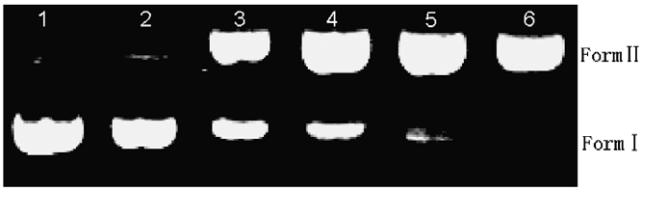

Figure 6. Electrophoretic separations of pBR322 DNA induced by $[Cu(dppz)(L\text{-trp})(H_2O)]ClO_4 \cdot C_2H_5OH \cdot H_2O$ at different concentrations in the presence of ascorbate in 5 mM Tris-HCl/50 mM NaCl buffer (pH = 7.2) at 298 K, $C_{DNA} = 300$ ng, $C_{ascorbate} : C_{complex} = 50 : 1$. Lane: (1) DNA alone, (2)–(6) DNA + ascorbate + the complex, $C_{Complex}$ (μM) = 1, 3, 5, 7, 9.

Table 3. Data of pBR322 DNA cleavage at different concentrations of the complex.

		Form (%)	
Serial no.[a]	Reaction condition	I	II
1	DNA control	94	6
2	DNA + 50 μM ascorbate + 1 μM the complex	85	15
3	DNA + 150 μM ascorbate + 3 μM the complex	37	63
4	DNA + 250 μM ascorbate + 5 μM the complex	27	73
5	DNA + 350 μM ascorbate + 7 μM the complex	18	82
6	DNA + 450 μM ascorbate + 9 μM the complex	5	95

[a]The serial number is the same as the lane number shown in figure 6.

The DNA cleavage efficiency of the complex was followed by monitoring the conversion of supercoiled (form I) closed circular plasmid DNA to the nicked circular (form II) or a linear (form III) species [38]. The plasmid pBR322 DNA cleavage induced by $[Cu(dppz)(L\text{-trp})(H_2O)]^+$ in the presence of ascorbate is shown in figure 6. The amounts of supercoiled, and nicked DNA quantified by densitometry are listed in table 3. The results indicate that, form I of pBR322 DNA decreases with increase in the concentration of the complex, and form II increases gradually under

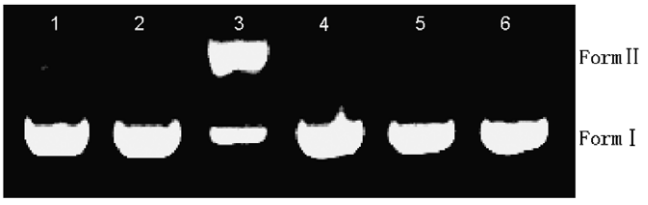

Figure 7. Electrophoretic separations of pBR322 DNA induced by different material. $C_{DNA} = 300$ ng, $C_{Complex} = C_{copper\ perchlorate} = C_{dppz} = 4\,\mu M$, $C_{ascorbate} : C_{complex} = 50:1$. Lane: (1) DNA alone, (2) DNA + [Cu(dppz)(L-trp)(H_2O)]$ClO_4 \cdot C_2H_5OH \cdot H_2O$, (3) DNA + [Cu(dppz)(L-trp)(H_2O)]$ClO_4 \cdot C_2H_5OH \cdot H_2O$ + ascorbate, (4) DNA + copper perchlorate + ascorbate, (5) DNA + dppz + ascorbate, (6) DNA +ascorbate.

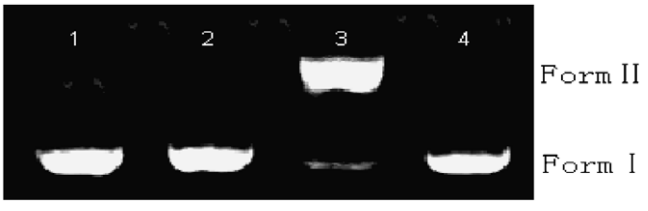

Figure 8. Cleavage of plasmid pBR322 DNA by [Cu(dppz)(L-trp)(H_2O)]$ClO_4 \cdot C_2H_5OH \cdot H_2O$ using inhibiton reagent DMSO. $C_{DNA} = 300$ ng, $C_{Complex} = 4\,\mu M$, $C_{ascorbate}$:$C_{Cu} = 50:1$, DMSO = 4 μM. Lane: (1) DNA alone, (2) DNA + DMSO, (3) DNA + [Cu(dppz)(L-trp)(H_2O)]$ClO_4 \cdot C_2H_5OH \cdot H_2O$ + ascorbate, (4) DNA + [Cu(dppz)(L-trp)(H_2O)]$ClO_4 \cdot C_2H_5OH \cdot H_2O$ + ascorbate + DMSO.

the conditions. The cleavage efficiency of the complex reached 95% at the concentration of 9 μM, but further increase in the concentration of the complex led to degradation of plasmid pBR322 DNA and no form I. The result is similar to that found for [{Cu(dppz)(DMF)}$_2$(μ-OH)$_2$](PF_6)$_2$ [39], indicating that the introduction of L-trp in the copper complex didn't give rise to selective interactions with DNA.

In order to clarify the preliminary mechanism of pBR322 DNA cleavage by the complex, further investigation was also carried out using Cu^{2+}, dppz, and ascorbate alone and [Cu(dppz)(L-trp)(H_2O)]$ClO_4 \cdot C_2H_5OH \cdot H_2O$ for reference (figure 7), and DMSO as inhibiting reagents (figure 8). Figure 7 showed that only the complex in the presence of ascorbate can convert the pBR322 DNA from form I to form II, and the other materials barely induce DNA strand cleavage. The results indicated that the complex plays an important role in cleavage of DNA. Moreover, it is evident that the hydroxyl radical scavenger DMSO diminished significantly the nuclease activity of the complex, which is indicative of the involvement of the radical in the cleavage process. Thus, a attacking mechanism of DNA by free hydroxyl radical induced by the complex is suggested [40].

4. Conclusions

A ternary Cu(II) complex with dipyrido[3,2-a : 2′3′-c]phenazine(dppz) and L-tryptophanate (L-trp) has been synthsized and structurally characterized. The complex binds to DNA *via* an intercalative mode and promotes the cleavage of plasmid pBP322 DNA in the presence of ascorbate.

Supplementary material

Detailed crystallographic data have been sent to the Cambridge Crystallographic Data Centre, 12 Union Road, Cambridge CB2 1EZ, UK, (Fax: +44-1223/336-033; Email: deposit@ccdc.cam.ac.uk) as supplementary material No. 271324 and can be obtained free of charge.

Acknowledgements

We thank the Natural Science Foundation of Guangdong Province (No. 04105986) and President Foundation of SCAU (No. 2003 × 004) for their financial support.

References

[1] K.E. Erkkila, D.T. Odom, J.K. Barton. *Chem. Rev.*, **99**, 2777 (1999).
[2] M.J. Clarke. *Coord. Chem. Rev.*, **236**, 209 (2003).
[3] A.A. Holder, S. Swavey, K. Brewer. *Inorg. Chem.*, **43**, 303 (2004).
[4] L.F. Tan, H. Chao, H. Li, Y.J. Liu, B. Sun, W. Wei, L.N. Ji. *J. Inorg. Biochem.*, **513**, 99 (2005).
[5] Y. Wu, H. Chen, P. Yang, Z. Xiong. *J. Inorg. Biochem.*, **99**, 1126 (2005).
[6] K. Karidi, A. Garoufis, N. Hadjiliadis. *J. Chem. Soc. Dalton Trans.*, 728 (2005).
[7] C.R. Mayer, E. Dumas, F. Secheresse. *Chem. Commun.*, 345 (2005).
[8] J.S. Kang, B.W. Son, H.D. Choi. *J. Biochem. Mol. Biol.*, **38**, 104 (2005).
[9] S. Dhar, A.R. Chakravarty. *Inorg. Chem.*, **44**, 2582 (2005).
[10] D.S. Sigman. *Biochemistry*, **29**, 9097 (1990).
[11] M. Chikira, Y. Tomizawa, D. Fukita, T. Sugizaki, N. Sugawara, T. Yamazaki, A. Sasano, H. Shindo, M. Palaniandavar, W.E. Antholine. *J. Inorg. Biochem.*, **89**, 163 (2002).
[12] S.C. Zhang, Y.G. Zhu, C. Tu, H.Y. Wei, Z. Yang, L.P. Lin, J. Ding, J.F. Zhang, Z.J. Guo. *J. Inorg. Biochem.*, **98**, 2099 (2004).
[13] H. Li, X.Y. Le, D.W. Pang, H. Deng, Z.H. Xu, Z.H. Lin. *J. Inorg. Biochem.*, **99**, 2240 (2005).
[14] R. Nagane, M. Chikira, M. Oumi, H. Shindo, W.E. Antholine. *J. Inorg. Biochem.*, **78**, 243 (2000).
[15] X.Y. Le, S.R. Liao, X.P. Liu, X.L. Feng. *J. Coord. Chem.*, **59** (2006), (In press).
[16] J.H. Kang, W.S. Eum. *Biochim. Biophys. Acta*, **1524**, 162 (2000).
[17] T. Sugimori, H. Masuda, N. Ohata, K. Koiwai, A. Odani, O. Yamauchi. *Inorg. Chem.*, **36**, 576 (1997).
[18] J.E. Dicken, L.A. Summers. *Aust. J. Chem.*, **23**, 1023 (1970).
[19] J. Marmur. *J. Mol. Biol.*, **3**, 208 (1961).
[20] M.E. Reichmann, S.A. Rice, C.A. Thomas, P. Doty. *J. Am. Chem. Soc.*, **76**, 3047 (1954).
[21] Brucker AXS, SAINT+ Version, 6.0, Brucker AXS, Madision, WI, USA (1999).
[22] R. Blessing. *Acta Crystallog.*, **A55,**, 33 (1995).
[23] A.J. Wilson. *International Tables for X-ray Crystallography*, Vol. C, Kluwer Academic Publishers, Dordrecht, 1992, Tables 6.1.1.4 (p. 500) and 4.2.6.8 (p. 219), respectively.
[24] G.M. Sheldrick. *SHELXS-97: Program for X-ray Crystal Structure Determination*, Göttingen University, Germany (1997).
[25] G.M. Sheldrick. *SHELXL-97: Program for X-ray Crystal Structure Refinement*, Göttingen University, Germany (1997).
[26] W.J. Gear. *Coord. Chem. Rev.*, **7**, 81 (1971).
[27] X.H. Zhou, X.Y. Le, S. Chen. *J. Coord. Chem.*, **58**, 993 (2005).
[28] Z.J. Song, X.Y. Le, H. Li, C.H. Liu, X.L. Feng. *Chin. J. Inorg. Chem.*, **21**, 527 (2005).
[29] K. Nakamoto. *Infrared and Raman Spectra of Inorganic and Coordination Compounds*, 4th Edn, p. 257, John Wiley and Sons Inc., New York (1986).
[30] S.A. Tysoe, A.D. Baker, T.C. Strekas. *J. Phys. Chem.*, **97**, 1707 (1993).
[31] P.S. Subramanian, E. Suresh, P. Dastidar, S. Waghmode, D. Srinivas. *Inorg. Chem.*, **40**, 4291 (2001).
[32] A. Wolfe, G.H. Shimer Jr, T. Meehan. *Biochemistry*, **26**, 6392 (1987).
[33] L. Changzheng, W. Jigui, W. Liufang, R. Min, J. Naiyong, G. Jie. *J. Inorg. Biochem.*, **73**, 195 (1999).
[34] A.M. Thomas, G. Neelakanta, S. Mahadevan, M. Nethaji, A.R. Chakravarty. *Eur. J. Inorg. Chem.*, **76**, 2720 (2002).

[35] J.R. Lakowicz, G. Webber. *Biochemistry*, **12**, 4161 (1973).
[36] S. Satyanaryana, J.C. Daborusak, J.B. Chaires. *Biochemistry*, **32**, 2573 (1993).
[37] S. Satyanaryana, J.C. Daborusak, J.B. Chaires. *Biochemistry*, **31**, 9319 (1992).
[38] J.K. Barton, A.L. Raphael. *J. Am. Chem. Soc.*, **106**, 2466 (1984).
[39] A.M. Thomas, M. Nethaji, A.R. Chakravarty. *J. Inorg. Biochem.*, **98**, 1087 (2004).
[40] J.K. Barton, A.T. Danishefsky, J.M. Goldberg. *J. Am. Chem. Soc.*, **106**, 2172 (1984).